Hierarchical Modeling of Polymer Electrolyte Membrane Fuel Cells

J. Dujc*[1], J.O. Schumacher[1]
[1]Zurich University of Applied Sciences
*Zurich University of Applied Sciences, ICP - Institute for Computational Physics
Wildbachstrasse 21, 8401 Winterthur, Switzerland, dujc@zhaw.ch

Abstract: A finite element model of a polymer electrolyte membrane fuel cell (PEMFC) is described in this paper. We divide the PEMFC into two separate and parallel 2D regions which are connected by the 1D regions representing the membrane electrode assembly (MEA). COMSOL Multiphysics was used as a development tool for hierarchical 1D MEA models. Here we present a 1D model that is based on seven governing equations describing the transport of the charges, heat, dissolved water, water vapor, hydrogen and oxygen. Extension of this model includes also the eight equation corresponding to the liquid water phase. Preliminary results of our simulations are also given.

Keywords: polymer electrolyte membrane fuel cell, PEMFC, membrane electrode assembly, MEA, modeling, model reduction, FEM.

1. Introduction

In the energy hungry modern world, the need to replace the fossil fuel based systems with sustainable and clean energy technologies is enormous. The leading replacement candidate in the transport applications as well as in stationary applications are the hydrogen fueled polymer electrolyte membrane fuel cells (PEMFC). In PEMFCs the chemical energy of hydrogen and oxygen is transformed into electricity, whereas the only byproduct is pure water.

The research and development of PEMFC systems is an ongoing process with an increasing demand for accurate numerical models. The two main obstacles when modeling the PEMFCs are: (i) the large area to thickness ratio of PEMFCs which makes a 3D analysis of the whole cell computationally very expensive and (ii) numerous coupled physical and electrochemical processes and solution variables which make the model very complex and numerically unstable. In order to tackle the first obstacle (i) we divided our model into a combination of two separated 2D regions, which are connected by the 1D regions, see [12]. The 2D regions capture all the significant in-plane phenomena, while the connecting 1D regions model the through-plane processes in the membrane electrode assembly (MEA). We tackle the second obstacle (ii) by carefully choosing which processes/fields are included in the model and what type of parameterization is used.

The rest of the paper is organized as follows. In Section 2, the governing equations are presented to model a membrane electrode assembly. Modeling in COMSOL Multiphysics is briefly explained. Preliminary results are presented in Section 3, and conclusions are drawn in Section 4.

2. 1D MEA models

The geometry of the membrane electrode assembly is shown in Fig. 1. It consists of 5 subdomains representing the anode side gas diffusion layer Ω_1, anode side catalyst layer Ω_2, membrane layer Ω_3, cathode side catalyst layer Ω_4 and cathode side gas diffusion layer Ω_5. The six boundaries are denoted with $\partial\Omega_i$, $i = 1,2,3,4,5,6$.

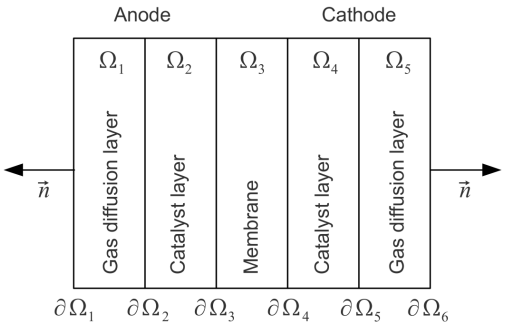

Figure 1: Geometry of the MEA model

2.1 Model with 7 fields

The behavior of the MEA can be described with varying level of complexity which is dependent on the number fields used and their type of parameterization. The following field variables are solved for: the electrostatic potential of electrons φ_e and protons φ_p, the temperature field T, the dissolved

water content of the membrane λ, the water vapor concentration c_v, the hydrogen concentration c_{O_2} and the oxygen concentration c_{H_2}. The general form of governing equation for each field can be described with the following partial differential equation

$$\nabla \cdot j_{field}^{\Omega_i} = q_{field}^{\Omega_i}, \tag{1}$$

where $j_{field}^{\Omega_i}$ is the flux, $q_{field}^{\Omega_i}$ is the source/sink term and the subscript $field$ denotes the fields $\varphi_e, \varphi_p, T, \lambda, c_v, c_{O_2}, c_{H_2}$. The superscript Ω_i denotes the subdomain as indicated in Fig. 1.

The field fluxes regions are

$$\begin{aligned}
j_e^{\Omega_i} &= -\sigma_e^{\Omega_i}\nabla\varphi_e, && i = 1,2,4,5,\\
j_p^{\Omega_i} &= -\sigma_p^{\Omega_i}\nabla\varphi_p, && i = 2,3,4,\\
j_T^{\Omega_i} &= -\kappa^{\Omega_i}\nabla T, && i = 1,2,3,4,5,\\
j_\lambda^{\Omega_i} &= n_{drag}\tfrac{j_p}{F} - \tfrac{{D_\lambda^{\Omega_i}}^{1.5}}{V_m}\nabla\lambda, && i = 2,3,4,\\
j_v^{\Omega_i} &= -D_v^{\Omega_i}\nabla c_v, && i = 1,2,4,5,\\
j_{O_2}^{\Omega_i} &= -D_{O_2}^{\Omega_i}\nabla c_{O_2}, && i = 4,5,\\
j_{H_2}^{\Omega_i} &= -D_{H_2}^{\Omega_i}\nabla c_{H_2}, && i = 1,2,
\end{aligned} \tag{2}$$

where i is the subdomain index, $\sigma_e^{\Omega_i}$ is the conductivity of the electron conducting phase, $\sigma_p^{\Omega_i}$ is the conductivity of the proton conducting phase, κ^{Ω_i} is thermal conductivity, $n_{drag} = \frac{2.5\lambda}{22}$ is the electroosmotic drag coefficient, F is Faraday's constant, $D_\lambda^{\Omega_i}$ is the dissolved water diffusion coefficient, V_m is the molar volume of the dry membrane, $D_v^{\Omega_i}$ is the water vapor Fickean diffusion coefficient, $D_{O_2}^{\Omega_i}$ is the oxygen effective diffusion coefficient, and D^{Ω_i} is the hydrogen effective diffusion coefficient. The nonzero source/sink terms related to the fluxes (2) are

$$\begin{aligned}
q_e^{\Omega_2} &= -Q^A, \quad q_e^{\Omega_4} = -Q^C,\\
q_p^{\Omega_2} &= Q^A, \quad q_p^{\Omega_4} = Q^C,\\
q_T^{\Omega_1} &= \sigma_e^{\Omega_1}\nabla{\varphi_e}^2,\\
q_T^{\Omega_2} &= -\tfrac{\Delta S^A T}{2F}\cdot Q^A + \eta^A \cdot Q^A + \sigma_e^{\Omega_2}\nabla{\varphi_e}^2 +\\
&\quad +\sigma_p^{\Omega_2}\nabla{\varphi_p}^2,\\
q_T^{\Omega_3} &= \sigma_p^{\Omega_3}\nabla{\varphi_p}^2,\\
q_T^{\Omega_4} &= -\tfrac{\Delta S^C T}{4F}\cdot Q^C + \eta^C \cdot Q^C + \sigma_e^{\Omega_4}\nabla{\varphi_e}^2 +\\
&\quad +\sigma_p^{\Omega_4}\nabla{\varphi_p}^2,\\
q_T^{\Omega_5} &= \sigma_e^{\Omega_5}\nabla{\varphi_e}^2,\\
q_\lambda^{\Omega_2} &= Q_{dv}, \quad q_\lambda^{\Omega_4} = Q_{dv} - \tfrac{Q^C}{2F},\\
q_v^{\Omega_2} &= -Q_{dv}, \quad q_v^{\Omega_4} = -Q_{dv},\\
q_{O_2}^{\Omega_4} &= \tfrac{Q^C}{4F},\\
q_{H_2}^{\Omega_2} &= -\tfrac{Q^A}{2F},
\end{aligned} \tag{3}$$

where Q^A and Q^C are the charge source/sink terms according to the Butler-Volmer equations, ΔS^A is the anode side reaction entropy, η_A is the anode overpotential, ΔS^C is the cathode side reaction entropy, η_C is the cathode overpotential and Q_{dv} is a source/sink term related to desorption and adsorption of dissolved water from and into the electrolyte. Note the substantial coupling of the fields in (3). The material and other parameters in (2) and (3) are generally not constants, but are rather functions of several field variables, which introduces additional coupling between the fields. For brevity, the full form of parameterization used in our simulations is omitted in this paper and we direct the reader to references [2], [3], [4], [5], [7], [8], [9], [11], [12], [13], [14], [16] for further discussion.

The partial differential equations (1), along with (2) and (3), are solved for the prescribed zero Neumann boundary conditions

$$(\vec{n}\cdot j_{field})|_{\partial\Omega_i} = 0, \tag{4}$$

where $\vec{n}$ denotes the outer normal at the subregion boundary $\partial\Omega_i$, and prescribed values of Dirichlet boundary conditions

$$field|_{\partial\Omega_i} = \overline{field}|_{\partial\Omega_i}, \tag{5}$$

where $\overline{field}|_{\partial\Omega_i}$ is the prescribed value of a field variable at the boundary $\partial\Omega_i$. The list of positions and accompanying fields with zero Neumann boundary conditions (4) used in our simulations is

$$\begin{aligned}
\partial\Omega_2: &\quad p, \lambda,\\
\partial\Omega_3: &\quad e, v, c_{H_2},\\
\partial\Omega_4: &\quad e, v, c_{O_2},\\
\partial\Omega_5: &\quad p, \lambda,
\end{aligned} \tag{6}$$

and the list with prescribed Dirichlet boundary conditions is

$$\begin{aligned}
\partial\Omega_1: &\quad e, T, v, c_{H_2},\\
\partial\Omega_6: &\quad e, T, v, c_{O_2}.
\end{aligned} \tag{7}$$

2.2 Model with 8 fields

The extension of the model described above includes also the field related to liquid water saturation s. The liquid water flux j_s is defined in the gas diffusion layers (Ω_1 and Ω_5) and in the catalyst layers (Ω_2 and Ω_4) and modeled according to Darcy's law [5]

$$j_s = -\frac{K_{abs}^{\Omega_i} K_{rel}}{\mu_w}\frac{\partial p_c}{\partial s}\nabla s, \tag{8}$$

where $K_{abs}^{\Omega_i}$ is the absolute permeability of the domain Ω_i, K_{rel} is the relative permeability, μ_w is the dynamic viscosity of liquid water and p_c is the capillary pressure. The relative permeability and the relationship between saturation s and capillary

pressure p_c are parametrized according to the Van Genuchten model [15], [6]

$$K_{rel}(s) = s^{\eta_k}\left(1-(1-s)^{1/m_k}\right)^{2m_k},$$
$$s(p_c) = 1-\left(1+\left(\frac{p_c+p_{atm}^{std}}{p_{cb}}\right)^{m}\right)^{-n}, \quad (9)$$

where η_k, m_k, p_{cb}, m and n are measurement fit parameters and p_{atm}^{std} is the standard atmospheric pressure. The source/sink terms related to water vapor in (3) no longer hold in this model. Instead, the liquid water and water vapor fields are coupled through phase change source and sink term Q_{pc} (see e.g. [10])

$$\begin{aligned} q_v^{\Omega_1} &= Q_{pc}, & q_s^{\Omega_1} &= -Q_{pc}, \\ q_v^{\Omega_2} &= Q_{pc}-Q_{dv}, & q_s^{\Omega_2} &= -Q_{pc}, \\ q_v^{\Omega_4} &= Q_{pc}-Q_{dv}, & q_s^{\Omega_4} &= -Q_{pc}, \\ q_v^{\Omega_5} &= Q_{pc}, & q_s^{\Omega_5} &= -Q_{pc} \end{aligned} \quad (10)$$

Zero Neumann boundary conditions for the liquid water field are assumed at $\partial\Omega_3$ and $\partial\Omega_4$ and prescribed Dirichlet boundary conditions are assumed at $\partial\Omega_1$ and $\partial\Omega_6$. currents

2.3 Use of COMSOL Multiphysics

The implementation starting point in COMSOL Multiphysics was the definition of geometry in Fig. 1. We further defined parameters and variables related to terms (2)-(3) and included seven General Form PDEs representing Eqns. (1). Each PDE was accompanied with appropriate Neumann and/or Dirichlet boundary conditions. With the model described in Section 2.1 we have performed an extensive parametric analysis, which was obtained by using the Parametric Sweep option in COMSOL Multiphysics.

In order to upgrade the COMSOL model from the formulation described in Section 2.1 to the formulation given in Section 2.2 we first introduce new parameters/variables for the description of terms (8)-(10). Further, one General Form PDE representing the liquid water field is added, source/sink terms are modified according to (10) and appropriate boundary conditions are defined.

3. Results

Here we present a small portion of results that we obtained with COMSOL Multiphysics 4.3 with the model presented in Section 2.1. In this example we varied the MEA boundary values of temperature, between 323 K and 363 K, and the molar fractions of oxygen and hydrogen of the supplying gas mixture, between 0.2 and 1. In Fig. 2 we present the current-voltage curves for four sets of boundary conditions. It can be seen that

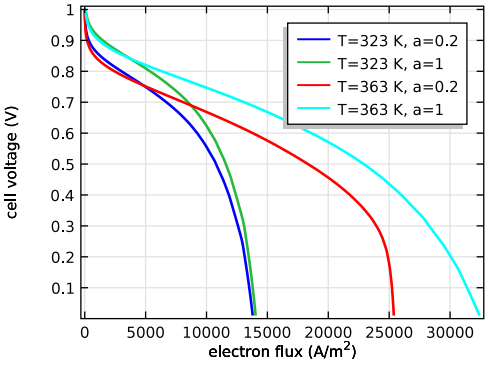

Figure 2: Current-voltage curves obtained with COMSOL Multiphysics 4.3 for varied boundary temperature conditions and molar fractions of oxygen and hydrogen of the supplying gas mixture.

at low current levels the increase of temperature slightly lowers the current, whereas for the currents greater the 5000 A/m^2, the fuel cell delivers more current at a specific voltage. The increase in the molar fractions leads to higher currents at a specific voltage. In the curve corresponding to higher boundary temperature and lower boundary molar fraction we can observe a mass-transport limitation, which is expressed by a very sharp decrease in voltage at around 25000 A/m^2.

4. Conclusion

The research and development of PEMFC numerical models is of great importance for the energy sustainable future. Our experience shows that COMSOL Multiphysics is a perfect testing ground for MEA model development. One can easily change the model and see the influence of a particular field/parameter on the results, which is a good guidance to what is important and which effects can be neglected in the model. We also use the COMSOL Multiphiysics results as a reference point for our in-house software SESES [1], which is later used to perform 2D+1D simulations on complex gas distribution flow-fields.

5. References

1. SESES Manual, http://icp.zhaw.ch/seses/ (2013)
2. O.S. Burheim, J.G. Pharoah, H. Lampert, P.J.S.

Vie, and S. Kjelstrup. Through-Plane Thermal Conductivity of PEMFC Porous Transport Layers, Journal of Fuel Cell Science and Technology, **8(2)**, 021013–1–021013–11 (2011)
3. R. Flückiger. Transport Phenomena on the Channel-Rib Scale of Polymer Electrolyte Fuel Cells, PhD thesis, ETH ZURICH (2009)
4. S. Ge, X. Li, B. Yi, and I-M. Hsing. Absorption, desorption, and transport of water in polymer electrolyte membranes for fuel cells, Journal of the Electrochemical Society,**152(6)**, A1149–A1157 (2005)
5. D. Gerteisen, T. Heilmann, and C. Ziegler. Modeling the phenomena of dehydration and flooding of a polymer electrolyte membrane fuel cell, Journal of Power Sources, 187:165–181 (2009)
6. J.T. Gostick, M.A. Ioannidis, M.W. Fowler, and M.D. Pritzker. Wettability and capillary behavior of fibrous gas diffusion media for polymer electrolyte membrane fuel cells Journal of Power Sources, **194(1)**, 433–444 (2009)
7. C.H. Hamann and W. Vielstich. Elektrochemie, WILEY-VCH, Weinheim, 3. edition (1998)
8. M. Khandelwal and M.M Mench. Direct measurement of through-plane thermal conductivity and contact resistance in fuel cell materials, Journal of Power Sources, **161**, 1106–1115 (2006)
9. C.K. Mittelsteadt and J. Staser. Simultaneous Water Uptake, Diffusivity and Permeability Measurement of Perfluorinated Sulfonic Acid Polymer Electrolyte Membranes, ECS Trans., **41(1)**, 101–121 (2011)
10. J.H. Nam and M. Kaviany. Effective diffusivity and water-saturation distribution in single- and two-layer PEMFC diffusion medium, International Journal of Heat and Mass Transfer, **46**, 4595–4611 (2003)
11. K.C. Neyerlin, G. Wenbin, J. Jorne, and H.A. Gasteiger. Determination of catalyst uniqe parameters for the oxygen reduction reaction in a PEMFC, Journal of the Electrochemical Society, **153(10)**, A1955–A1963 (2006)
12. J.O. Schumacher, J. Eller, G. Sartoris, T. Colinart, and B. Seyfang. 2+1D modelling of a polymer electrolyte fuel cell with glassy-carbon micro-structures, Mathematical and Computer Modelling of Dynamical Systems, **DOI:10.1080/13873954.2011.642390**, 1–23 (2012)
13. T.E. Springer, T.A. Zawodzinski, and S. Gottesfeld. Polymer electrolyte fuel cell model, Journal of the Electrochemical Society, **8(138)**, 2334–2341 (1991)
14. H. Wu. Mathematical modeling of transient transport phenomena in PEM fuel cells, PhD thesis, University of Waterloo (2009)
15. N. Zamel, X. Li, J. Becker, and A. Wiegmann. Effect of liquid water on transport properties of the gas diffusion layer of polymer electrolyte membrane fuel cells, International Journal of Hydrogen Energy, **36(9)**, 5466–5478 (2011)
16. C. Ziegler. Modeling and Simulation of the Dynamic Behavior of Portable Proton Exchange Membrane Fuel Cells, PhD thesis, Universität Konstanz (2005)

6. Acknowledgements

The authors gratefully appreciate financial support from the Swiss Federal Office of Energy SFOE.